Computer modelling of $BaLiF_3$: I. Interionic potentials and intrinsic defects

1996 J. Phys.: Condens. Matter 8 10931

(http://iopscience.iop.org/0953-8984/8/50/019)

J. Phys.: Condens. Matter **8** (1996) 10931–10937. Printed in the UK

Computer modelling of $BaLiF_3$: I. Interionic potentials and intrinsic defects

R A Jackson†, M E G Valerio‡ and J F de Lima‡

† Department of Chemistry, Keele University, Keele, Staffs ST5 5BG, UK
‡ Departamento de Física, CCET, UFS, 49.100-000 São Cristóvão-SE, Brazil

Received 7 August 1996

Abstract. A computational study of $BaLiF_3$ is presented. Interionic potentials are fitted to experimental data and the resulting potentials used to calculate the defect behaviour. Energies of formation of basic defects are obtained and used to predict intrinsic disorder and to calculate activation energies for ion migration. This information is used to suggest the possible mechanisms involved in the ionic conductivity of the material.

1. Introduction

$BaLiF_3$ is a material which adopts the inverted perovskite structure (see figure 1). It has interesting properties as a potential laser material and this behaviour depends on its defect properties. Computer modelling methods provide a means of studying defect properties and of gaining information which may be difficult to obtain experimentally.

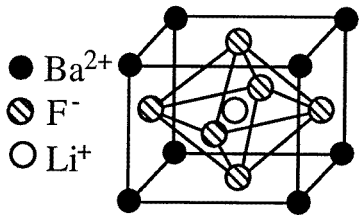

Figure 1. The $BaLiF_3$ structure.

The material has been the subject of a number of experimental studies. Haussühl *et al* [1] measured a number of properties, including the lattice parameter, unit cell density and elastic constants. Boumriche *et al* [2] performed infrared dielectric dispersion measurements, obtaining dielectric constants and frequencies of infrared-active modes. These authors also commented on the high stability of $BaLiF_3$ relative to those of the other AMF_3 fluoroperovskites.

Concerning the potential laser properties of the material, these depend on doping with divalent transition metal ions. Prado *et al* [3] have studied the optical properties of Pb^+ centres in $BaLiF_3$ and Martins *et al* [4] have studied Ni^{2+} doping. Finally, Duarte *et al* [5] have considered $BaLiF_3$:Co^{2+}. These results suggest that the material can be used as a vibronic laser in the infrared region.

0953-8984/96/5010931+07$19.50

In the present paper, a computer modelling study of the perfect and defect properties of $BaLiF_3$ is presented. As well as calculating the intrinsic defects, ion migration energies have been calculated with a view to predicting the ionic conductivity of the material.

2. The computational method

2.1. Energy minimization

The computational method used in this paper is based on lattice energy minimization, in which the material is described in terms of ions interacting through effective potentials. Having specified these potentials, the lattice energy of the material is minimized by varying the structural parameters (atomic positions and unit cell constants). Values of physical properties of the lattice, such as elastic and dielectric constants, are calculated for the minimum energy structure. Essential pre-requisites are the interionic potentials, and their determination is described in section 2.2. All calculations were performed using the General Utility Lattice Program (GULP) [6].

2.2. Interionic potentials

For ionic materials, the interactions responsible for cohesion are (i) electrostatic interactions between ions and (ii) short-range attractive and repulsive interactions due respectively to van der Waals forces and electron charge cloud overlap. These interactions are embodied in the Buckingham potential, supplemented by an electrostatic term:

$$V(r) = q_1 q_2/r + A\exp(-r/\rho) - Cr^{-6}$$

where q_1 and q_2 are charges of ions 1 and 2, r is their separation, and A, ρ and C are parameters to be fitted.

Another feature of ionic crystals is the importance of ionic polarizability, especially for anions, to which the outer electrons may be less strongly bound. This feature can be represented by the shell model, in which the ion is described by a core and a shell, coupled by a harmonic spring. The ion mass is concentrated on the core, and the charge is partitioned between core and shell. In the Buckingham potential, if one or both of the ions are represented by the shell model, the interactions are calculated between shells. The ionic polarizability (α) is related to the shell charge (Y) and the harmonic spring constant (k) as follows:

$$\alpha = Y^2/k.$$

The interionic potentials used in the calculations were obtained by empirical fitting, in which the potential parameters are adjusted until the structure and lattice properties are reproduced satisfactorily by the potential. The procedure is explained in figure 2. For $BaLiF_3$, the potential was fitted to the following properties: (i) the crystal structure, (ii) atomic positions, (iii) elastic constants (c_{11}, c_{12} and c_{44}) and (iv) dielectric constants (both static and high-frequency ones). Table 1 gives a comparison of the calculated and experimental constants. It is seen that very good agreement is obtained, while noting that the splitting of c_{12} and c_{44} is not reproduced by our potential, which is a general feature of central force models. However, the experimental values of the elastic constants c_{12} and c_{44} are seen to be very close to the calculated ones.

The potential parameters obtained from the fitting are given in table 2. It is to be noted that cation–cation interactions were not parameterized since these interactions are

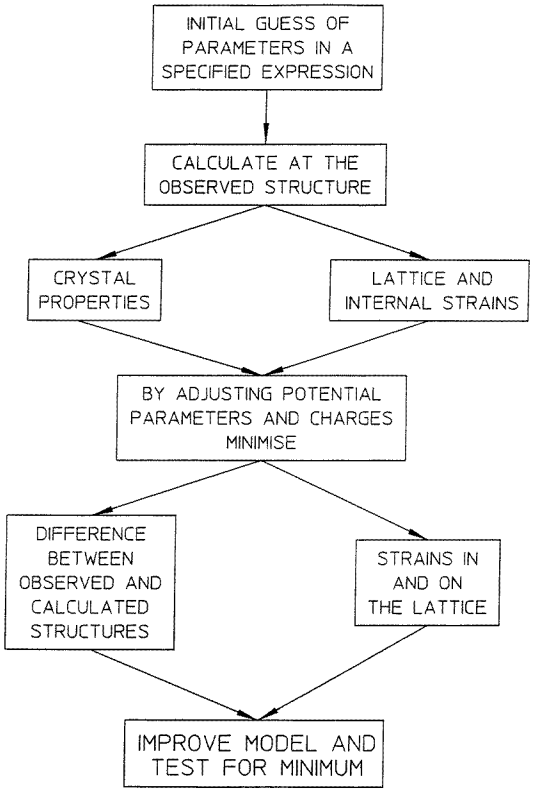

Figure 2. The calculational procedure.

Table 1. Perfect lattice properties for $BaLiF_3$.

Constant	Calculated	Experimental	Reference
Lattice energy (eV)	−34.83		
Lattice parameter			
a (Å)	3.995	3.995	[3]
Unit cell density			
ρ (g cm^{-3})	5.242	5.238	[1]
Elastic constants (dyn cm^{-2})			
c_{11}	12.99	12.98	[1]
c_{12}	4.76	4.65	[1]
c_{44}	4.76	4.87	[1]
Dielectric constants			
ε_0	11.70	11.71	[2]
ε_∞	2.25	2.25	[2]

predominantly electrostatic. A shell model description is used for the anion but not for the cations; excellent agreement with the high-frequency dielectric constants shows that this is justified.

Table 2. Potential parameters obtained by empirical fitting.

Short-range interactions	A (eV)	ρ (Å)	C (eV Å^6)
Ba_{core}–F_{shell}	3090.2	0.2987	0.0
Li_{core}–F_{shell}	400.6	0.2736	0.0
F_{shell}–F_{shell}	1153.0	0.1365	0.0
Shell model parameters			
$Y = q(F_{shell}) = -2.321\|e\|$			
$k(F_{core} - F_{shell}) = 48.40$ eV Å^{-2}			

2.3. Modelling of defects

Having represented the perfect lattice, defects are introduced using the Mott–Littleton approximation [7, 8], in which a spherical region of lattice surrounding the defect is treated explicitly, namely all interactions are considered (region I), and more distant parts of the lattice are treated as a dielectric continuum (region IIB). There is an interface region (region IIA) which ensures a smooth transition between the explicitly summed and continuum regions. Care must be taken in ensuring that region I is large enough for the defect energy to converge.

In the calculations reported, region I sizes of 10 Å were used and the region IIA radius was 15 Å. In terms of numbers of ions, this corresponds to about 300 in region I and 850 in region IIA The short-range potential cut-off was 10 Å.

3. Results

3.1. Basic defects

Energies of formation of basic defects are given in table 3. The defects are defined using Kroger–Vink notation. Three different interstitial sites have been considered for all the ions; the positions are shown in figure 3. Note that position $(\frac{1}{2}\,0\,0)$ is at the centre of the edge of the cube formed by the Ba ions, position $(\frac{1}{2}\,\frac{1}{4}\,\frac{1}{4})$ is at the centre of the edge of the octahedron of F ions, and position $(\frac{1}{4}\,\frac{1}{4},\,\frac{1}{4})$ is on the diagonal of the cube formed by the Ba ions. Also given in table 3 are the lattice energies of BaF_2 and LiF, which are needed in the calculation of intrinsic defect energies.

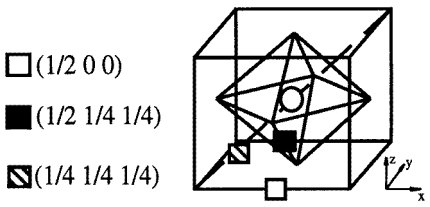

Figure 3. The three considered interstitial sites.

In discussing the results it is first to be noted that the F interstitial at $(\frac{1}{2}\,\frac{1}{4}\,\frac{1}{4})$ did not converge, indicating that this is not a stable position for F. This is not surprising since this position is very close to two other F positions, leading to strong repulsion. The other results are used to calculate intrinsic defect energies, as discussed in the next section.

Table 3. Basic defect energies.

Defect		Energy of formation (eV)
$V_F^{\cdot}$		4.13
F_i'	$(\frac{1}{2}\,0\,0)$	−0.46
	$(\frac{1}{4}\,\frac{1}{4}\,\frac{1}{4})$	−0.81
V_{Ba}''		18.86
$Ba_i^{\cdot\cdot}$	$(\frac{1}{2}\,0\,0)$	−8.32
	$(\frac{1}{2}\,\frac{1}{4}\,\frac{1}{4})$	−8.53
	$(\frac{1}{4}\,\frac{1}{4}\,\frac{1}{4})$	−7.77
V_{Li}'		8.51
$Li_i^{\cdot}$	$(\frac{1}{2}\,0\,0)$	−4.91
	$(\frac{1}{2}\,\frac{1}{4}\,\frac{1}{4})$	−4.69
	$(\frac{1}{4}\,\frac{1}{4}\,\frac{1}{4})$	−5.32
Li_{Ba}'		11.47
$Ba_{Li}^{\cdot}$		−4.20
Lattice energies for associated fluorides E_l (eV)		
BaF_2		−23.13
LiF		−10.18

3.2. Intrinsic defects

Energies of formation of intrinsic defects are given in table 4. The Frenkel and $BaLiF_3$ Schottky energies are defined in the usual way, but the pseudo-Schottky energies for BaF_2 and LiF are calculated according to the reactions below, and the Jackson–Lima–Valerio (JLV) defect corresponds to exchange of Ba and Li between their respective sites:

$$Li_{Li}+F_F \rightarrow V_{Li}'+V_F^{\cdot}+LiF$$
$$Ba_{Ba}+2F_F \rightarrow V_{Ba}''+2V_F^{\cdot}+BaF_2.$$

It can be seen that the most favourable type of disorder corresponds to creation of pseudo-Schottky LiF defects; however, the F and Li Frenkel energies are also relatively low, so this type of disorder might be found at higher temperatures. This suggests that the material is likely to be highly defective. Ion migration is considered in the next section.

3.3. Ion migration

It is first necessary to consider the possible mechanisms by which ions can migrate through the $BaLiF_3$ lattice. The possible mechanisms are as follows.

(i) *The vacancy mechanism*

(a) F: the ion migrates via a neighbouring vacancy site.

(b) Li: there are two possibilities here. The first involves migration via a nearest-neighbour vacant Li site, which is nonlinear because there is a F ion in the centre of the face shared by both cubes containing the Li sites. The second is a linear jump to the next-nearest-neighbouring Li site; in this situation there is no ion blocking the path.

Table 4. Intrinsic defect energies per defect.

	Interstitial site	Frenkel energies (eV)		Schottky energies (eV)
F	$(\frac{1}{2}\,0\,0)$	3.67	$BaLiF_3$	4.93
	$(\frac{1}{4}\,\frac{1}{4}\,\frac{1}{4})$	3.32	Pseudo-Schottky BaF_2	3.99
			Pseudo-Schottky LiF	2.46
Li	$(\frac{1}{2}\,0\,0)$	3.60		
	$(\frac{1}{4}\,\frac{1}{4}\,\frac{1}{4})$	3.82		JLF energy
	$(\frac{1}{4}\,\frac{1}{4}\,\frac{1}{4})$	3.19		(eV)
Ba	$(\frac{1}{2}\,0,\,0)$	10.54	$Ba_{Li} + Li_{Ba}$	7.27
	$(\frac{1}{2}\,\frac{1}{4}\,\frac{1}{4})$	10.33		
	$(\frac{1}{4}\,\frac{1}{4}\,\frac{1}{4})$	11.09		

Table 5. Ion migration energies.

Mechanism	$E_{cluster}$ (eV)	$E_{activation}$ (eV)
Vacancy		
F	4.39	0.26
Li (linear)	11.81	3.30
Li (nonlinear)	11.92	3.42
Interstitial		
F	−0.46	0.35
Li (via $(\frac{1}{2}\,0\,0)$)	−4.91	0.41
Li (via $(\frac{1}{2}\,\frac{1}{4}\,\frac{1}{4})$)	−4.69	0.63
Interstitialcy		
Li (collinear)	−5.314	0.003
Li (non-collinear)	−5.112	0.205

(ii) *The interstitial mechanism*

(a) F: an ion at the interstitial site $(\frac{1}{4}\,\frac{1}{4}\,\frac{1}{4})$ migrates to a symmetrically equivalent site via the interstitial site at $(\frac{1}{2}\,0\,0)$.

(b) Li: there are two possibilities which have been considered here. The first one is equivalent to the F interstitial mechanism. The second involves an ion at the interstitial site $(\frac{1}{4}\,\frac{1}{4}\,\frac{1}{4})$ migrating to a symmetrically equivalent site but this time via the interstitial site at $(\frac{1}{2}\,\frac{1}{4}\,\frac{1}{4})$.

(iii) *The interstitialcy mechanism*

This has only been considered for the case of the Li ion, and there are two possibilities. In both cases a Li ion at $(\frac{1}{4}\,\frac{1}{4}\,\frac{1}{4})$ moves to the centre of the cube, where it displaces the ion at that site to another interstitial site symmetrically equivalent to $(\frac{1}{4}\,\frac{1}{4}\,\frac{1}{4})$. The difference between the two is that in one case the two ions move along one cube diagonal (a linear mechanism), whereas in the other case the ions move along different diagonals, leading to a V-shaped mechanism.

Energies for all the above processes are given in table 5. The activation energies are calculated as follows: in each case, the migration mechanism is modelled by setting

up a system involving the migrating ion(s) at their saddle point. The energy for this configuration is defined as $E_{cluster}$ in table 5. It should be noted that the migrating ion and surrounding ions were allowed to relax in calculating this energy. The activation energy, $E_{activation}$, is obtained by taking into account the overall process; for example, for the vacancy mechanism, the formation energy of the vacancy is subtracted from the cluster energy to give the activation energy.

From these results it is clear that, for F migration, the vacancy mechanism and the interstitial mechanism have similar activation energies, so that it might be expected that either mechanism would occur. However, for Li migration, the vacancy mechanism is not favoured and, provided that there are Li interstitials present, the collinear interstitialcy mechanism has lowest energy and will dominate the Li migration process in $BaLiF_3$.

4. Conclusions

In this paper the derivation of an empirical potential for $BaLiF_3$ has been reported, which gives excellent agreement with available experimental data. This potential has then been used to calculate the energies of formation and migration of defects in the material.

Concerning the energies of formation of defects, it can be concluded that the most likely intrinsic defect disorder will involve formation of Li and F vacancy pairs, but that, at higher temperatures, Li and F Frenkel pairs might be formed since their energies are also relatively low. Ion migration will depend on the intrinsic disorder, so if the information from sections 3.2 and 3.3 is combined, the following can be concluded.

(i) At low temperatures, the dominant process will be F migration by the vacancy mechanism, so that ionic conductivity at these temperatures might be due mainly to F.

(ii) At higher temperatures, the existence of Li and F interstitials may lead to Li migration by the collinear interstitialcy mechanism, and F migration by the interstitial mechanism, so that there may be additional contributions to the conductivity from these processes.

A consequence of these results is that it is possible that $BaLiF_3$ might exhibit properties similar to those of a superionic conductor. This possibility will be examined experimentally in the near future and may form the basis of a future publication.

Acknowledgments

The authors would like to thank the Conselho Nacional de Desenvolvimento Científico e Tecnológico (CNPq) and the Brazilian Physical Society (SBF) for financial support, and the EPSRC (UK) and CESUP (Brazil) for computing facilities. The GULP code was written by Dr Julian Gale (IC, London) and we are grateful for permission to use it in this work.

References

[1] Haussühl S, Leckebusch R and Recker K 1972 *Z Naturf.* a **27** 1022–4
[2] Boumriche A, Simon P, Rousseau M, Gesland J Y and Gervais F 1989 *J. Phys.: Condens. Matter* **1** 5613–20
[3] Prado L, Vieira N D Jr, Baldochi S L and Morato S P 1993 *Solid State Commun.* **87** 41–6
[4] Martins E, Vieira N D Jr, Baldochi S L and Morato S P 1994 *J. Lumin.* **62** 281–9
[5] Duarte M, Martins E, Baldochi S L, Vieira N D Jr and Vieira M M F 1995 *Pesq. Desenv. Tecnol.* **19** 24–5
[6] Gale J D 1992–6 *General Utility Lattice Program (GULP)* (London: Royal Institution/Imperial College)
[7] Mott N F and Littleton M J 1938 *Trans. Faraday. Soc.* **34** 485
[8] Catlow C R A 1989 *J. Chem. Soc. Faraday Trans.* II **85** 335–40